Sustainable Horizons 7 (2023) 100060

Contents lists available at ScienceDirect

Sustainable Horizons

journal homepage: www.elsevier.com/locate/horiz

Original Research Articles

Assessment of Bitcoin carbon footprint

Samuel Asumadu Sarkodie [a,*], Mohammad Amin Amani [b], Maruf Yakubu Ahmed [c], Phebe Asantewaa Owusu [a]

[a] Nord University Business School (HHN). Post Box 1490, 8049 Bodø, Norway
[b] School of Industrial and Systems Engineering, College of Engineering, University of Tehran, Tehran, Iran
[c] Accounting and Finance, University of Vaasa, Wolffintie 32, FI-65200 Vaasa PO Box 700, 65101 Vaasa, Finland

ARTICLE INFO

Keywords:
Proof-of-work
Bitcoin blockchain
Carbon footprint
Bitcoin energy consumption
Cryptocurrency

ABSTRACT

Bitcoin is a breakthrough financial technology but a volatile asset in financial markets with a complex fundamental consensus algorithm (Proof-of-Work) limiting its large-scale adoption due to environmental-related issues. Hitherto, the role of its technical and infrastructural composition that drives carbon footprint from an ecological perspective is rarely discussed in the literature. Here, we use machine learning and econometric techniques to analyze the past, present, and future changes in Bitcoin's carbon footprint with daily data spanning July 18, 2010 to December 04, 2021. We document technical drivers, decomposition effects, causal nexus, and implications of the Bitcoin blockchain's increasing energy and carbon footprint. We show that Bitcoin's technical drivers could have potential impacts on Bitcoin's carbon footprint, and subsequently, global climate change. For example, the network's hashrate increases mining difficulty—thereby increasing Bitcoin's energy consumption and subsequently, carbon footprint. We observed a direct association between the marginal effect of block size and transaction count—implying that a higher block size improves transaction efficiency and then reduces Bitcoin's energy and carbon footprint. Besides, low mining difficulty increases market capitalization whereas increasing mining difficulty reduces bitcoin mining profit in the long run. This infers the reward for mining Bitcoin has a diminishing return in the long term. Thus, the adoption of advanced hardware for Bitcoin mining will spur energy and carbon intensity, yet will have a low return on investment. We highlight environmental regulations and regulatory changes that could limit Bitcoin's carbon footprint.

1. Introduction

The world's most popular cryptocurrency, viz., Bitcoin has increasingly been criticized in recent years due to its high energy use generated mainly from fossil fuels. This technological breakthrough is not only limited to its medium of exchange but the underlining blockchain technology—where network participants validate transactions via a decentralized distributed ledger protocol (Stoll et al., 2019). However, the mining of Bitcoin through a proof-of-work (PoW) consensus network creates massive carbon emissions due to the staggering amount of energy consumption (Digiconomist, 2022). Global adoption of cryptocurrency surged by ~880% from July 2020 to June 2021 just within a span of one year (CMC, 2022). In January 2009, the first Bitcoin was minted with the objective of providing reliable and faster digital payment without reliance on central banks (Nakamoto, 2008). In this context, the decision to validate transactions through the PoW consensus mechanism by Satoshi Nakamoto is delegated to the network participants. Unlike fiat currency, a transaction in Bitcoin depends on the computational power expended to solve complex algorithmic challenges tracked through the public ledger of decentralized computers worldwide called a blockchain (Nakamoto, 2008). The total computational power used each second to process the PoW blockchain mined is known as the hashrate. This mechanism ensures the security and stability of the network, because of the large computer infrastructure and the significant amount of energy required to achieve consensus, hence, making it more difficult for malicious participants to force an invalid ledger (O'Dwyer et al., 2014). The participants who submit blocks to the network to form the distributed ledger technology (DLT) are known as miners (Köhler et al., 2019). The miners add the next group of transactions to the block and receive compensation in the form of newly minted coins and collect fees for transactions within the block (O'Dwyer et al., 2014). However, a block is rejected when it contains invalid transactions which implies the validator receives no reward and thus, incurs a net loss for the expended computing power and energy

* Corresponding author.

https://doi.org/10.1016/j.horiz.2023.100060
Received 10 May 2023; Received in revised form 5 June 2023; Accepted 11 June 2023
Available online 16 June 2023

consumed (IMF, 2022).

The PoW consensus mechanism requires enormous energy for validation than most countries, which industry players refer to as Bitcoin's "Achilles heel" (Baur et al., 2022). From an environmental perspective, Bitcoin mining has negative implications in two ways namely carbon emissions from high energy use and electronic waste from numerous large computer infrastructures. These limiting factors of the public DLT involve mining rigs competing to solve complex energy-intensive cryptographic puzzles in a winner-takes-all race. For example, the annual energy consumption of the Bitcoin mining network is ~144 terawatt hours (TWh) per year accounting for 0.6% of the total global electricity use as of April 2022 (IMF, 2022). The annual electricity use of crypto-assets grew by ~67% from July 2021 to January 2022, before declining by ~17% by August 2022. Bitcoin accounts for ~60% of the total global energy use by cryptocurrencies whereas Ethereum accounts for ~20% (WHG, 2022). Global annual electronic transactions in 2017 stood at ~US$314.2 billion, of which Bitcoin transactions accounted for only ~0.033% with corresponding energy use emitting more than 69 $MtCO_{2eq}$ emissions (Mora et al., 2018; WB, 2018). In recent years, cryptocurrencies particularly Bitcoin—once a fringe asset class, have experienced exponential global adoption in the mainstream by major companies and financial firms (Iyer, 2022). Great demand comes with higher prices, as thousands of miners use increasingly energy-intensive computers to compete in solving cryptographic puzzles in the fastest time to get rewards—as the cryptographic problem adjusts regularly to become more difficult to ensure that each miner on the average of every 10-minutes produces one valid block (O'Dwyer et al., 2014). The PoW economic model generally suggests that the network consumes more electricity as the value of Bitcoin grows and the distribution of the coins among miners stays constant (Coin Desk, 2022). For example, in November 2021 the all-time-high price of Bitcoin was US$68,000 per coin at a market capitalization of ~US$1.2 trillion (Sarkodie et al., 2022).

Despite the potential for rapid crypto market growth, future energy demand from PoW operations are uncertain. The electricity usage of crypto-miners changes in response to fluctuations in market capitalization, and the adoption of new components and technologies. Although direct comparisons are complicated, bank electronic payment such as Visa Card, MasterCard, and American Express reported a combined electricity consumption of ~0.5 kWh inclusive of all electronic payment and operational systems in 2020 (American Express, 2021; Master Card, 2021; Visa, 2020). These three companies combined use only ~1% electricity that Bitcoin and Ethereum consumed per year (Digiconomist, 2022). Additionally, evidence from existing literature suggests that the global banking sector including not only the data centers, but the branches, Automated Teller Machines (ATMs), and a range of trusted third parties consumes about 650 TWh while Bitcoin mining consumes 144 TWh annually (De Vries, 2019; McCook, 2014). In 2018, the global banking sector processed ~482.6 billion non-cash transactions compared to the Bitcoin network with nearly 81.4 million processed transactions per annum (Capgemini, 2018). This major difference in transactions is due to the limited scalability of Bitcoin. For example, Bitcoin's block limit of 1 megabyte of data prevents the network from processing more than 7 transactions per second—which theoretically infers ~220 million annual transactions against the nearly 700 billion annual processed transactions of the global financial system (Digiconomist, 2022).

Bitcoin is a volatile asset in financial markets with a complex fundamental consensus algorithm limiting its large-scale adoption due to environmental-related issues. Several studies have investigated the relationship between Bitcoin and carbon emissions. For example, findings on the relationship between Bitcoin, carbon credit, and the green energy sector highlight the significant influence of Bitcoin energy consumption on the performance of the energy industry (Corbet et al., 2021). However, another study suggests that renewable energy is not the answer to the Bitcoin sustainability problems as the energy used is not the only avenue in which mining affects the environment (De Vries, 2019). Existing literature suggests that the rate of Bitcoin adoption broadly based on current technologies could create electricity consumption capable of producing emissions that may trigger a global temperature above 2 °C in a few decades (Mora et al., 2018). Evidence from previous studies suggests Bitcoin and Ethereum have a causal effect on environmental degradation (Erdogan et al., 2022). Another study estimated that energy consumed in mining US$1 of Bitcoin is about four-fold in mining US$1 of copper but double what is used in mining US $1 of gold (Stoll et al., 2019). Besides, the energy footprint of Bitcoin PoW far exceeds that of all proof-of-stake (PoS) based systems by about three times (Platt et al., 2021).

However, the role of Bitcoin's technical and infrastructural composition that drives carbon footprint from an ecological perspective is rarely discussed in the literature. Analyzing Bitcoin's carbon footprint is crucial for environmental regulation and policy. Here, we identify Bitcoin's emission sources and measure its carbon output and the potential impact on climate change. We use machine learning and econometric techniques to analyze the past, present, and future changes in Bitcoin's carbon footprint with daily data spanning July 18, 2010 to December 04, 2021. We document the technical drivers, decomposition effects, causal nexus, and implications of increasing energy and carbon footprint of Bitcoin transactions. The decomposition properties are examined using the wavelet technique to assess the temporal evolution of non-periodic and transitory characteristics of Bitcoin's carbon footprint and technical drivers. We use the wavelet technique due to its inherent characteristics for short-lived transient factors permitting the assessment of steady change in drivers of Bitcoin's carbon footprint (Lau et al., 1995; Mallat, 1999). We employ the time-varying Granger causality with a recursive rolling window testing technique to assess the predictive power of drivers underpinning Bitcoin's carbon footprint while accounting for their temporal stability using historical dynamics (Shi et al., 2020). This technique enables the accounting of time-frequency variations and the timing of changes using date-stamping scenarios to produce unbiased statistical inferences. We further investigate the causal nexus while accounting for potential heterogeneity, market volatility, and complexities of Bitcoin's carbon footprint and technical drivers. We use a machine learning-based regression model that controls for misspecification bias while producing consistent results with fitted values that fulfill normality assumptions—by learning the data generation procedure, model-derived causal inferences, and prediction regardless of its functional form (Hainmueller et al., 2014). Finally, we use deep learning that encompasses a wide range of algorithms including deep neural networks, and convolutional neural networks. We apply the convolutional Long short-term memory which combines both convolutional neural network (i.e., extracts spatial features using convolutional operations) and long short-term memory (i.e., a recurrent neural network that extracts time characteristics using memory units and doors) algorithms in the extraction of both spatial and temporal characteristics (Wang et al., 2022).

2. Methods

2.1. Data

We employed a daily frequency dataset spanning July 18, 2010 to December 4, 2021 (4158 observations), which captures earlier recorded and reported daily transactions of bitcoin on crypto exchanges. Our dataset comprises technical indicators (i.e., mining, network usage, transactions, addresses, and market measures) of the Bitcoin network including the mean difficulty (dimensionless), mean hashrate (varies, rate), mean block size (bytes), sum of active count of addresses (addresses), sum of count of transactions (transactions), market capitalization (US$) (Coin Metrics, 2022), optimal bitcoin electricity consumption (kWh) (CBECI, 2021) and optimal bitcoin carbon footprint ($kgCO_2$) (Sarkodie and Owusu, 2022). The market capitalization

measures the total market value of circulating bitcoin supply (i.e., the current price of bitcoin × circulating bitcoin supply). Bitcoin energy use entails the total annualized electricity use of the BTC network based on a 7-day moving average less reliant on short-term hashrate variabilities (CBECI, 2021). Bitcoin's carbon footprint captures the optimal carbon emissions from the bitcoin network assuming electricity is derived from coal, oil, and gas sources (Sarkodie and Owusu, 2022). The mean difficulty measures the effort of finding a unique protocol-designated required hash (i.e., the difficulty of mining a new block) at a given interval. The difficulty is periodically adjusted (2016 blocks, or nearly every two weeks) by the Bitcoin protocol as a function of the amount of hashing power deployed by miners (Coin Metrics, 2022). The mean hashrate measures the rate at which Bitcoin miners solve hashes at specific intervals. Thus, captures the computational speed across all Bitcoin miners in the network (Coin Metrics, 2022). The block size captures all mean daily created blocks whereas addresses measure the sum count of unique and active addresses (i.e., originator or recipient of a ledger change) in the Bitcoin network (Coin Metrics, 2022). Transactions measure the sum count of a collection of intended actions to alter the user-initiated ledger but excluding authorized protocol changes to the ledge (Coin Metrics, 2022).

$$R_{x,y}(\alpha,\tau)=\frac{\| \langle W_{x,y}(\alpha,\tau)\rangle \|}{\| \langle W_{x,x}(\alpha,\tau)\rangle \|^{1/2}\| \langle W_{y,y}(\alpha,\tau)\rangle \|^{1/2}} \tag{1}$$

2.2. Generalized KPSS stationarity test

Analyzing the stationarity properties of sampled series is crucial to the adoption of robust estimation techniques while curtailing spurious regression and biased inferences. Contrary to the existing Phillips-Perrons (PP) and Dickey-Fuller (DF) unit root tests that are weak in assessing the stationarity properties of highly autoregressive and near-integrated data (DeBoef et al., 1997), we employed a modified test version of Kwiatkowski et al. (1992) [KPSS used hereafter]. Though the traditional KPSS test is more robust compared to PP and DF techniques—yet, in highly autoregressive data, the traditional KPSS test is prone to higher type-1 error rates (Kagalwala, 2022). The modified version of the KPSS test [i.e., generalized KPSS (GKPSS used hereafter)] utilizes Quadratic Spectral Kernel and Automatic Bandwidth Lag selection technique for lag truncation, hence, producing lower prevalence rates of type-1 errors in restricted samples (Hobijn et al., 2004).

2.3. Wavelet analysis

After confirming the nonstationary process among sampled series, we examined the decomposition properties of Bitcoin's carbon footprint versus technical indicators (addresses, block size, market capitalization, difficulty, hashrate, and transaction count) while accounting for daily frequency localization. The decomposition properties of wavelet transform [i.e., signal decomposition of narrow and wide wavelets (functions) in high-frequency and low-frequency characteristics] leads to an optimal time-scale (daily frequency) resolution useful for assessing the temporal evolution of nonperiodic and transitory signals (Lau et al., 1995; Mallat, 1999). We used the wavelet technique due to its inherent characteristics (i.e., characterize nonstationary signals of bivariate time series) for short-lived transient factors permitting the assessment of steady change in drivers of Bitcoin's carbon footprint. Thus, using the wavelet technique allows for unearthing useful information along the daily time scale of fluctuations in Bitcoin's carbon footprint. While there are several types of wavelets, this study employed the complex continuous wavelet (i.e., Morlet wavelet) which controls for noise, hence, producing robust phase relationships between bivariate time series compared to other existing forms of wavelets. The association between nonstationary bivariate signals [$x(t)$ and $y(t)$] can be quantified using wavelet cross-spectrum [$W_{x,y}(\alpha,\tau)=W_x(\alpha,\tau)\,W_y^{*}(\alpha,\tau)$] and coherence function expressed as (Cazelles et al., 2008):

Where the wavelet coherency [$R_{x,y}(\alpha,\tau)$] is deduced by normalizing the wavelet cross-spectrum [$W_{x,y}(\alpha,\tau)$] by the spectrum of both bivariate signals while controlling scale factor [α] and time shift [τ]. $\langle..\rangle$ represents the time and scale bound smoothing operator. The phase interactions between bivariate signals [$x(t)$ and $y(t)$] can be examined by using the phase difference expressed as (Cazelles et al., 2007):

$$\psi_{x,y}(\alpha,\tau)=\tan^{-1}\frac{\Im\left(\langle W_{x,y}(\alpha,\tau)\rangle\right)}{\Re\left(\langle W_{x,y}(\alpha,\tau)\rangle\right)} \tag{2}$$

Where the phase difference [$\psi_{x,y}(\alpha,\tau)$] is proportional to the ratio of the imaginary part [$\Im$] and real part [$\Re$] of the wavelet cross-spectrum [$W_{x,y}(\alpha,\tau)$] of both signals.

2.4. Econometrics of Bitcoin

We further assessed the predictive power of drivers underpinning Bitcoin's carbon footprint while accounting for their temporal stability using historical dynamics. Contrary to the sensitivity of previous causality tests to the time period, we employed the time-varying Granger-causality (TVGC) with recursive testing techniques (Shi et al., 2020). Due to the volatility of the price of bitcoin, failing to account for time-frequency variations and timing of changes via date stamping produces biased and inaccurate information for statistical inferences. The rolling window (RoW) algorithm is used for statistical inferences by generating the test statistics for each computed time period (Arora et al., 2016). The RoW algorithm used in this study entails a window size (T_w) of 832 (20% of sampled observations) rolled through the sampled data ($T+1$) for each timely observation ($y_0,\ \ldots\ y_T$) identified and a corresponding computed Wald test ($\mathscr{T}_{r1,\,r}$) for each window (Schwarz, 1978). Thus, each $\mathscr{T}_{r1,\,r}$ with a subsample $r_1=r-w$ and $r\in|r_0,\ 1|$ is computed from a same T_w ($0<w<1$), and size sample of 365 observations included in the 500 bootstrapped iterations with 2 lags (i.e., selected using Akaike information criterion), and 1 lag augmentation of the VAR model while accounting for heteroskedasticity robustness (Swanson, 1998). To test the null hypothesis of no causality from the individual predictors (y_{2t}) to bitcoin carbon footprint (y_{1t}), we first fitted a bivariate vector autoregressive (VAR) model expressed as:

$$\begin{vmatrix} y_{1t} \\ y_{2t} \end{vmatrix}=\begin{vmatrix} \varnothing_{11}^{(1)} & 0 \\ \varnothing_{11}^{(2)} & \varnothing_{21}^{(2)} \end{vmatrix}\begin{vmatrix} y_{1,\,t-1} \\ y_{2,\,t-1} \end{vmatrix}+\begin{vmatrix} \varepsilon_{1t} \\ \varepsilon_{2t} \end{vmatrix} \tag{3}$$

Where $\varnothing_{11}^{(1)}$, $\varnothing_{11}^{(2)}$, and $\varnothing_{21}^{(2)}$ are the estimated coefficients and residuals are represented by e_{1t} and e_{2t}. The bootstrapped sample series is computed as (Baum et al., 2022):

$$\begin{vmatrix} y_{1t}^{b} \\ y_{2t}^{b} \end{vmatrix}=\begin{vmatrix} \widehat{\varnothing}_{11}^{(1)} & 0 \\ \widehat{\varnothing}_{11}^{(2)} & \widehat{\varnothing}_{21}^{(2)} \end{vmatrix}\begin{vmatrix} y_{1,\,t-1}^{b} \\ y_{2,\,t-1}^{b} \end{vmatrix}+\begin{vmatrix} \varepsilon_{1t}^{b} \\ \varepsilon_{2t}^{b} \end{vmatrix} \tag{4}$$

Where bootstrapped sample size is represented by $T_b=\tau_0+\tau_b-1$,

$\tau_0 = \mathscr{T}_{r0}$, $\tau_b = \mathscr{T}_{rb}$, the residuals ($e^b_{1t}$ and e^b_{1t}) are drawn randomly and replaced sequentially from the estimated residuals using initial values (y^b_{11} and y^b_{21}) from the estimated y_{11} and y_{21}. The test statistic ($\left[\mathscr{T}^b_{t-\tau_0+1,t}\right]_{t=\tau_0}^{\tau_0+\tau_b-1}$) for the RoW algorithm is estimated using the bootstrapped sample series y^b_{1t} and y^b_{2t}. The cycle from Eq. (4) is repeated $b = 1, \ldots, B$ times. The 90th, 95th, and 99th percentiles are estimated using the 90, 95, and 99% critical values from B bootstrapped computed test statistics. The extended procedure of the algorithm is presented in Ref. (Baum et al., 2022). The timing of changes for potential causal nexuses is identified using date stamping output in plots with corresponding critical values aka percentiles.

Next, we examined the heterogeneous effects of bitcoin's addresses, block size, market capitalization, difficulty, hashrate, and transaction count on its carbon footprint using kernel regularized least squares (KRLS)—a machine learning-based regression model that accounts for challenges with classification and heterogeneity without assuming linearity or additivity (Hainmueller et al., 2014; Sarkodie et al., 2020). Though without assuming a strong parametric presupposition, the KRLS approach produces unbiased (by controlling for misspecification bias) and consistent results while fulfilling normality assumptions. Due to market volatility and complexities of the bitcoin blockchain and related technical infrastructure, we used the KRLS algorithm to learn the procedure for data generation, model-derived causal inferences, and prediction even without correct or unknown functional form (Hainmueller et al., 2014). The procedure of the KRLS algorithm involves (a) the estimation of pointwise and average marginal effects using a standardized dataset, automatic regularization parameter, and kernel bandwidth, (b) hypothesis testing along with confidence interval construction, and (c) validating the model for consistent, and unbiased results while fitted values are normally distributed (Ferwerda et al., 2017).

2.5. Deep learning of Bitcoin

The deep learning of Bitcoin's carbon and energy footprint was preceded by the Min-Max normalization of the dataset. The features of the dataset have different ranges, so features contributing to model fitting and learning have bias. Therefore, to preprocess the dataset, a normalization technique was applied. Min-Max normalization is one of the proper methods that can solve the problem of model overfitting and learning bias by converting the data values to decimals between 0 and 1. This method scales the features by the formulation presented in Eq. (5) as:

$$X_{scaled} = \frac{X - F_{min}}{F_{max} - F_{min}} \tag{5}$$

where X_{scaled} is the new measure of X, F_{min} is the minimum quantity in feature F, and F_{max} is the maximum value in feature F.

The other preprocessing step applied to the dataset involves converting the time series data to supervised learning, which makes the data appropriate for training deep learning models. In this approach, the previous multistep of the target variable and its current step turned into a sequence. In other words, the target variable at the time step (t) of the output is predicted based on the inputs of its previous steps ($t - 1, \ldots, t - n$) (Brownlee, 2017). This preprocessing function is just applied to the target variable (bitcoin's carbon and energy footprint) because the analysis is a univariate time series.

In machine learning, deep learning encompasses a wide range of algorithms, including deep neural networks, recurrent neural networks, and convolutional neural networks Amani and Marinello, 2022). A convolutional neural network (CNN) extracts spatial features using convolutional operations (Amani and Sarkodie, 2022), while Long short-term memory (LSTM)—a type of recurrent neural network extracts time characteristics using memory units and doors. In contrast, convolutional LSTM (ConvLSTM) applies both algorithms in the extraction of both spatial and temporal characteristics (Wang et al., 2022). The essential formulations of the ConvLSTM architecture are expressed in Eqs. (6–(10) (Shi et al., 2015).

$$i_t = \sigma\left(W_{xi} * X_t + W_{hi} * H_{t-1} + W_{ci} \odot C_{t-1} + b_i\right) \tag{6}$$

$$f_t = \sigma\left(W_{xf} * X_t + W_{hf} * H_{t-1} + W_{cf} \odot C_{t-1} + b_f\right) \tag{7}$$

$$C_t = f_t \odot C_{t-1} + i_t \odot tanh(W_{xc} * X_t + W_{hc} * H_{t-1} + b_c) \tag{8}$$

$$o_t = \sigma\left(W_{xo} * X_t + W_{ho} * H_{t-1} + W_{co} \odot C_t + b_0\right) \tag{9}$$

$$H_t = o_t \tanh(C_t) \tag{10}$$

where * indicates the convolution operator, H_t represents a hidden state, f_t represents a forgotten door, X_t represents the input, b denotes the bias, i_t represents an input door, $\odot$ indicates Hadamard product, C_t represents a cell state, o_t represents an output door, and W represents a filter. The essential parts of ConvLSTM are the convolution of memory units and doors. C_t stores status information as an accumulator while adaptive training parameters are used to control the door. The input door (i_t) accumulates the data associated with each new input in the memory unit (C_{t-1}). The forget gate (f_t) determines whether a cell state of the past (C_{t-1}) will be "forgotten" during this sequence. Output gate (o_t) determines whether the final unit output will be entered into the final state. The 1D vector (f_t, i_t, o_t) in typical LSTM loses information when processing space-time data, but the ConvLSTM vector has three dimensions. Therefore, ConvLSTM extracts spatial features as well as time-to-time characteristics with convolution operations. Fig. 1(a) shows the inner structure of the ConvLSTM model.

Several techniques and features can be added to Bitcoin's carbon and energy footprint models to increase its performance. An activation function called the rectified linear unit (ReLU) applies non-linearity to a network, which assists in producing the non-linearity boundaries (Agarap, 2018). As a result of introducing this non-linearity to our networks, the accuracy of the ConvLSTM algorithm is significant and evident. The formulation of the ReLU activation function can be expressed as:

$$ReLU = Max\ (0,\ x) \tag{11}$$

Dropout is a method that ignores a percentage of neurons that have been randomly selected. Therefore, on the forward propagation, the contributions of these neurons are removed temporally, and weight updates are not applied (Srivastava et al., 2014). By using this technique, overfitting (i.e., the model learned well but can't predict appropriately) can be curtailed. The final scheme of the models is presented in Fig. 1(b).

We use the root mean squared logarithmic error (RMSLE) as the performance evaluation metric to assess the deep learning model. RMSLE is the root mean squared error (RMSE) of the log-transformed predicted and log-transformed real values. RMSLE is an appropriate metric when the problem has exponential growth. This metric measures the ratio of predicted and real values. RMSLE formulation is mentioned in Eq. (12) as:

$$RMSLE = \sqrt{\frac{1}{n}\sum_{i=1}^{n}\left(\log(p_i + 1) - \log(r_i + 1)\right)^2} \tag{12}$$

where p_i is the prediction of the dependent variable, r_i is the real value of the dependent variable, and n is the number of observations.

3. Results

We used transformed data series to ensure the probability density function of the sampled variables is not far from Gaussian (Grinsted et al., 2004). Normally distributed series (i.e., the Jarque-Bera test

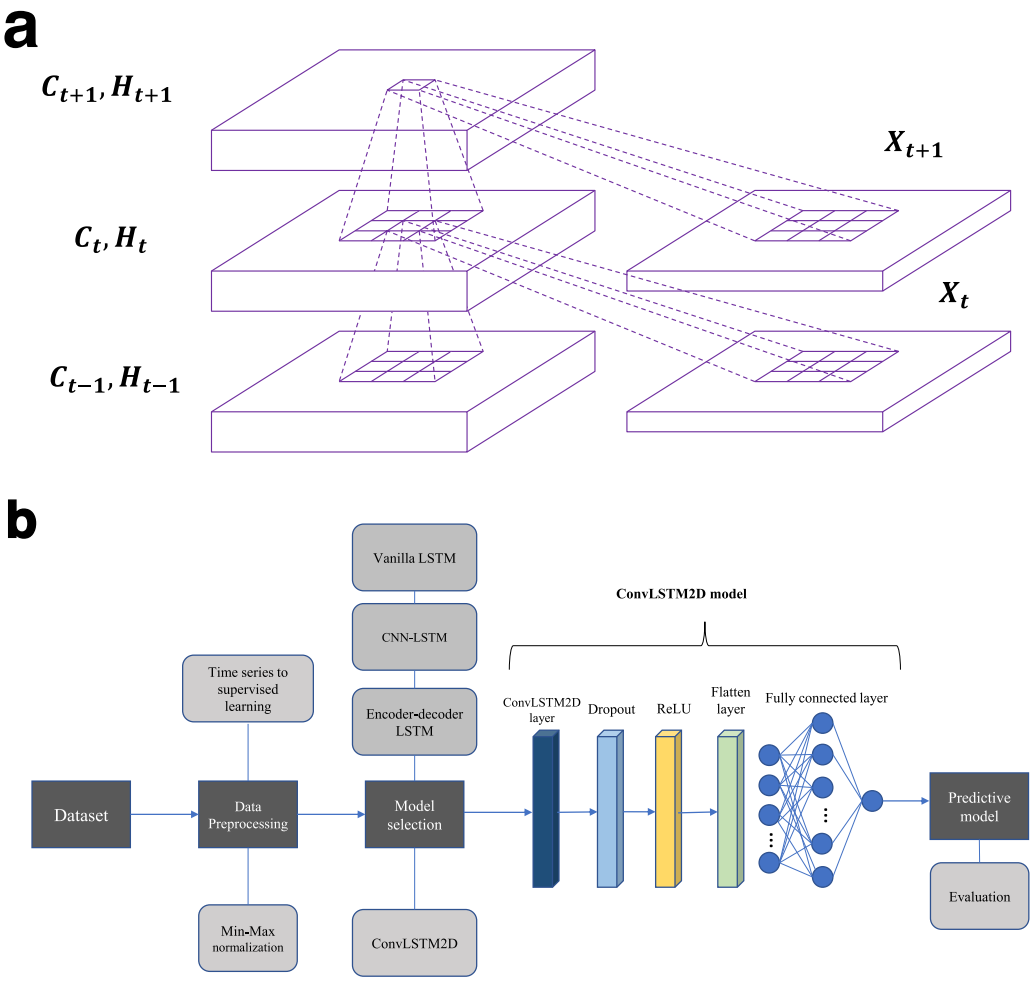

Fig. 1. Supervised learning of Bitcoin carbon and energy footprint (a) The ConvLSTM inner structure (Shi et al., 2015) (b) Schematic representation of the model.

rejects the null hypothesis of normality, justifying the data transformation) produce more reliable and statistically significant wavelet results (see Supplementary Table 1). Similarly, the stationarity of data series was investigated using the novel generalized KPSS (GKPSS) test based on a quadratic spectral kernel, and automatic bandwidth lag truncation with 7 lags. The GKPSS test strongly rejects the null hypothesis that all series are trend-stationary. Besides, the graphical plot shows a log-transformed trend of data series in levels. Thus, both the results and time series plot validate the nonstationary behavior of sampled variables (see Supplementary Table 2; Supplementary Fig. 1). The estimated wavelet coherence via the cross-wavelet bias-corrected method presented in Fig. 2 was computed from 2000 Monte Carlo randomizations. The dark-red areas signify the high interrelation between the *x* and *y* series whereas the dark-blue areas denote lower dependency between the *x* and *y* series. The gray-dotted lines represent the cone of influence (COI) delimiting regions not induced by edge effects. The phase plots show black arrows pointing left (which indicates both *x* and *y* series are in anti-phase), right (which implies both *x* and *y* series are in phase), downward (which infers *x* leads *y* by $\pi/2$), and upward (which shows *y* leads *x* by $\pi/2$). There exist areas of sparse-phase relationship between technical indicators (addresses, block size, market capitalization, difficulty, and transaction count) excluding hashrate and bitcoin carbon footprint. The phase nexus of both technical indicators (excluding hashrate) and Bitcoin carbon footprint shows in phase behavior (Fig. 2(a-b, d-f)). Hashrate has a strong and high interrelation with Bitcoin's carbon footprint in both high and low scales spanning all time periods. Fluctuations in hashrate are exhibited in bitcoin carbon footprint wavelengths spanning 2010 to 2021. The phase nexus shows both hashrate and bitcoin carbon footprint are in phase whereas hashrate leads bitcoin carbon footprint by 90° and vice versa (Fig. 2(c)).

Subsequently, we used the TVGC technique with a rolling window algorithm to examine the temporal causality between technical indicators and Bitcoin carbon footprint while identifying periods (using a date-stamping method) where the nexus varies significantly. We used the AIC information criteria to select an optimal lag to ensure robust temporal causality tests. The TVGC test entails a minimum of 832 observations as initialization window size with 6 lags, 500 replications, and a controlled size of 365 days. Both upper and lower dashed lines depicted in Fig. 3 denote 5% and 10% bootstrapped critical values (see Supplementary Table 3). The computed maximum Wald rolling test statistic exceeds the 90th-99th percentile from the bootstrapped empirical distribution test (Supplementary Table 3). The TVGC robust test statistics reject the null hypothesis of no causality from difficulty, hashrate, block size, tx count, and market capitalization to bitcoin carbon footprint at 5% significance level (however, causality from addresses to bitcoin carbon footprint is acceptable at 10% level). The time-varying Granger causality plots in Fig. 3 show dynamic relationships with corresponding patterns of causality including from 18-Jan-2012 to 04-Dec-2021. The plots further show evidence of Granger causality whenever the solid line (denoting the test statistic) exceeds the dashed lines (denoting the bootstrapped empirical distribution test). There is strong evidence ($p<0.001$) of global shocks from the COVID-19 pandemic that led to economic recession occurring on March 12, 2020 (Sarkodie et al., 2022). This perhaps increased global adoption of cryptocurrencies, specifically bitcoin—which increased energy consumption (and subsequently bitcoin carbon footprint) due to increased

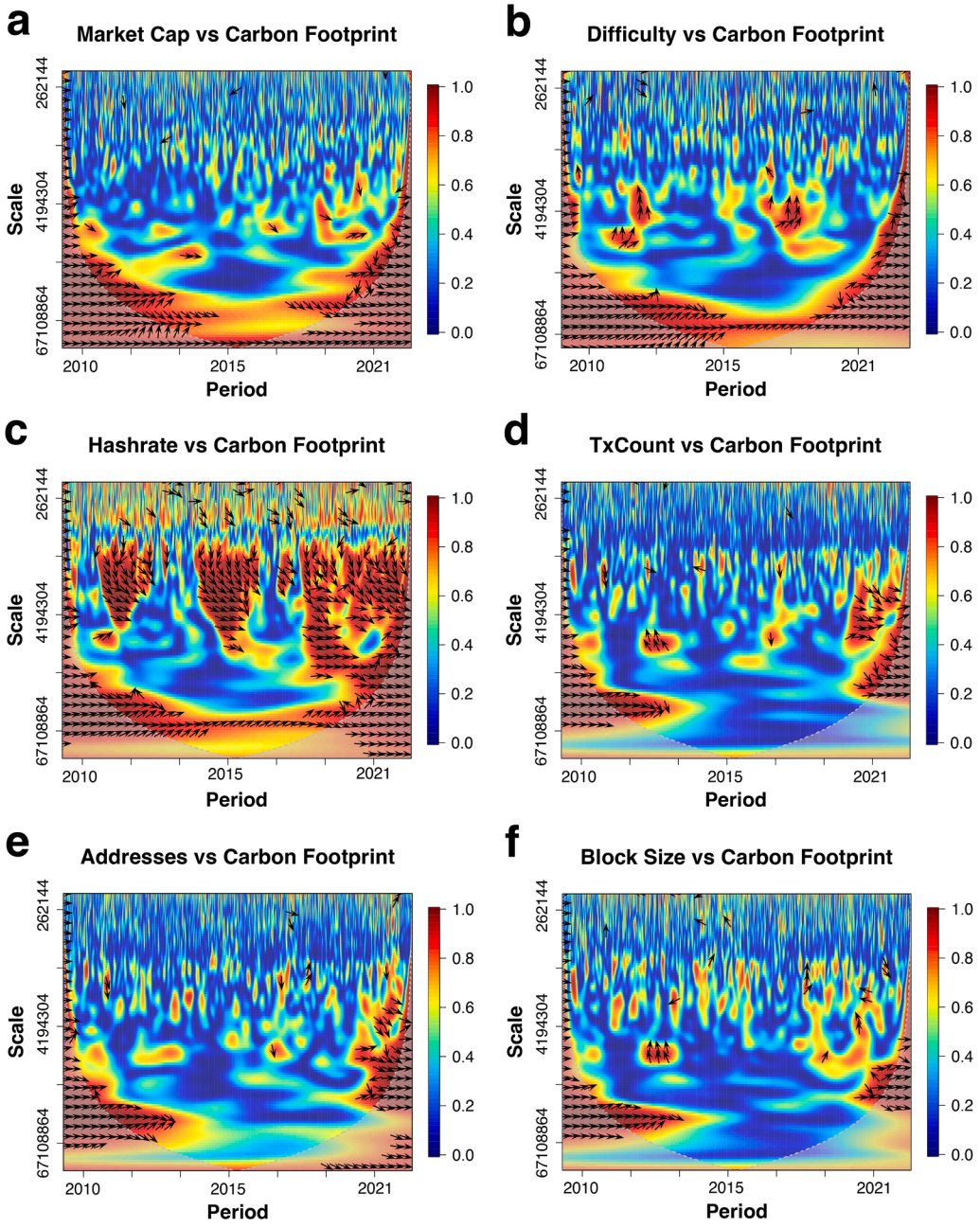

Fig. 2. Wavelet analysis of Bitcoin carbon footprint versus (a) Market capitalization (b) Difficulty (c) Hashrate (d) Tx count (e) Addresses (f) Block size. Estimated wavelet coherence via the cross-wavelet bias-corrected method computed from 2000 Monte Carlo randomizations. The dark red areas signify the high interrelation between the *x* and *y* series whereas the dark blue areas denote lower dependency between the *x* and *y* series. The gray-dotted lines represent the cone of influence (COI) delimiting regions not induced by edge effects. The phase plots show black arrows pointing left (indicates both *x* and *y* series are in anti-phase), right (implies both *x* and *y* series are in phase), downward (infers *x* leads *y* by $\pi/2$), and upward (shows *y* leads *x* by $\pi/2$).

outputs in bitcoin mining difficulty, hashrate, block size, tx count, and market capitalization. However, there is little evidence ($p<0.10$) of the role of addresses in affecting Bitcoin's carbon footprint (Supplementary Fig. 2(*e*)). The recursive-evolving window algorithm further shows evidence of Granger causality from block size and market capitalization to Bitcoin carbon footprint spanning late 2017 to 2021 (Supplementary Fig. 2(*c,f*)). These causality findings and the strong correlation (Fig. 4 (a)) show difficulty, hashrate, block size, tx count, and market capitalization are closely linked to Bitcoin's carbon footprint, hence, can predict future energy and emission dynamics.

Next, we examined the causal effects of Bitcoin's carbon footprint by using a machine learning-based regression technique and a subsequent prediction using a neural network. Residuals of the parameter estimates are robust and stable, without challenges with structural breaks (Supplementary Fig. 3(*a-h*)). The pointwise estimation shows the marginal effects of market capitalization, addresses, difficulty, hashrate, and transaction count are significantly ($p<0.05$) positive whereas block size is significantly ($p<0.05$) negative (Fig. 4). We observe that market capitalization has the highest probability of increasing Bitcoin's carbon footprint by 0.41 percentage points. Hashrate, addresses, difficulty, and transaction count are associated with ~0.05–0.10 percentage point probability of escalating Bitcoin's carbon footprint. In contrast, block size is the only technical driver with mitigating effects on Bitcoin's carbon footprint by a probability of 0.17 percentage points. Increasing the block size will result in more transactions processed per block—which will cause fewer blocks to be mined, thus, reducing both Bitcoin energy and carbon footprint. To identify the potentiality of nonlinearity and interactive effects among the technical drivers, we regressed the pointwise partial derivatives (from the KRLS model) of each independent variable on the raw variables (original dataset). We find evidence of statistically significant interactive effects and nonlinearities among Bitcoin technical indicators (Supplementary Tables 4–9). This further confirms the association between market capitalization, addresses, difficulty, hashrate, block size, and transaction count that explains the

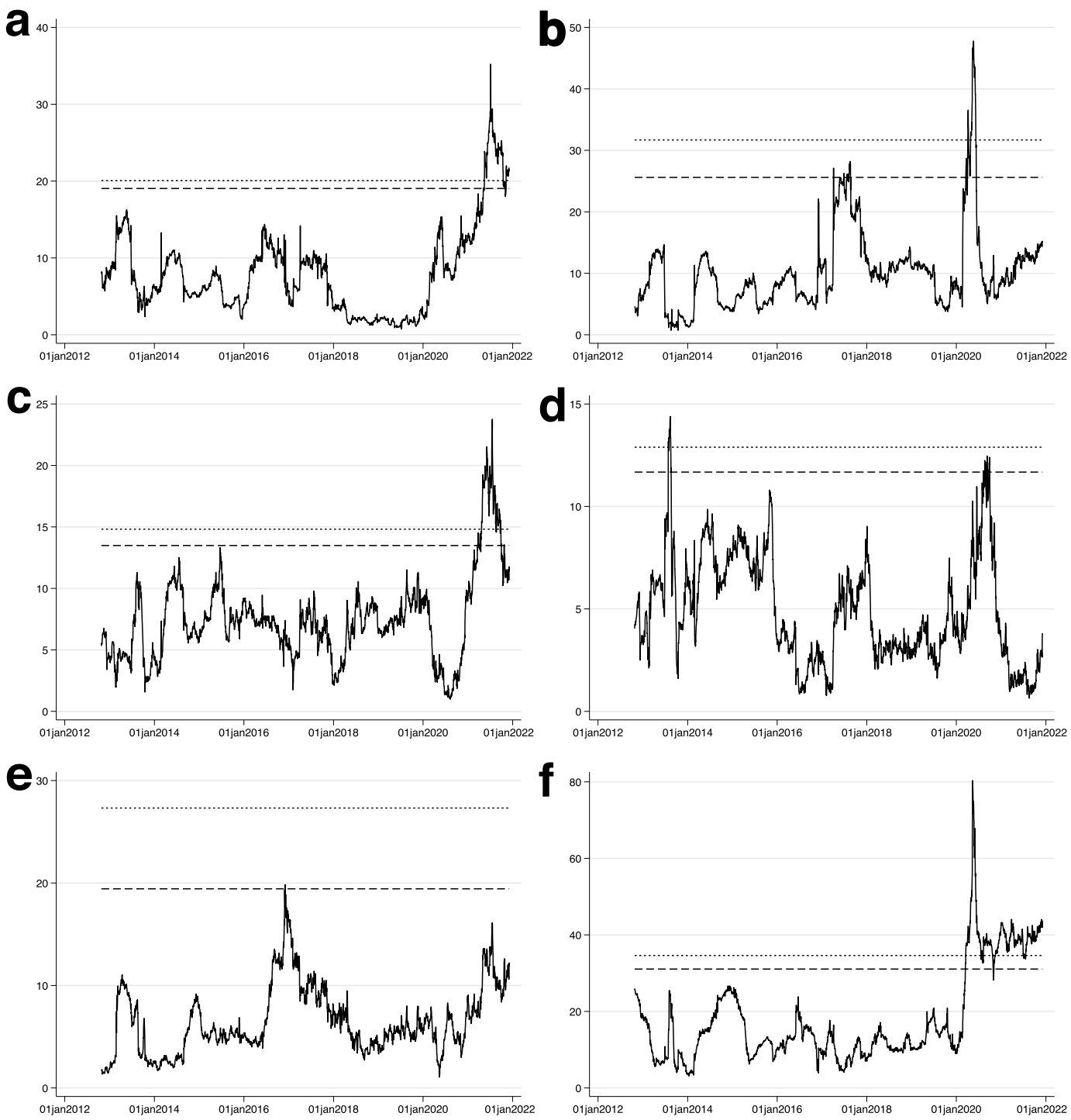

Fig. 3. Time-varying causality using rolling window algorithm. (a) Difficulty (b) Hashrate (c) Block size (d) Tx count (e) Addresses (f) Market capitalization. Time-varying LA-VAR Granger causality test including trend from 18-Jul-2010 to 04-Dec-2021. Both upper and lower dashed lines denote 5% and 10% bootstrapped (with 6 lags, 500 replications, minimum of 832 observations as window size, and 365 days as control size) critical values. The TVGC robust test statistics reject the null hypothesis of no causality based on the 90th-99th percentile of test statistics. The estimated Wald test statistics are robust to heteroskedasticity.

dynamics and changes in Bitcoin's carbon footprint. For example, we observe strong evidence of a positive monotonic relationship between the marginal effect of both hashrate and difficulty (Supplementary Fig. 4 (*a*)), validating the nearly perfect correlation in Fig. 4(a). This implies that as the network's hashrate increases, the bitcoin mining difficulty increases—thereby increasing energy consumption and subsequently, carbon footprint. We further show that low mining difficulty resulted in increased market capitalization whereas an increase in mining difficulty will make bitcoin mining unprofitable in long term (Supplementary Fig. 4(*b*)). This infers that advanced hardware, more energy use, and carbon footprint will increase, yet with a low return on investment. We observe a direct association between the marginal effect of block size and transaction count, as the limit of the block size determines the number of transactions per block (Supplementary Fig. 4(*d*)). Thus, a higher block

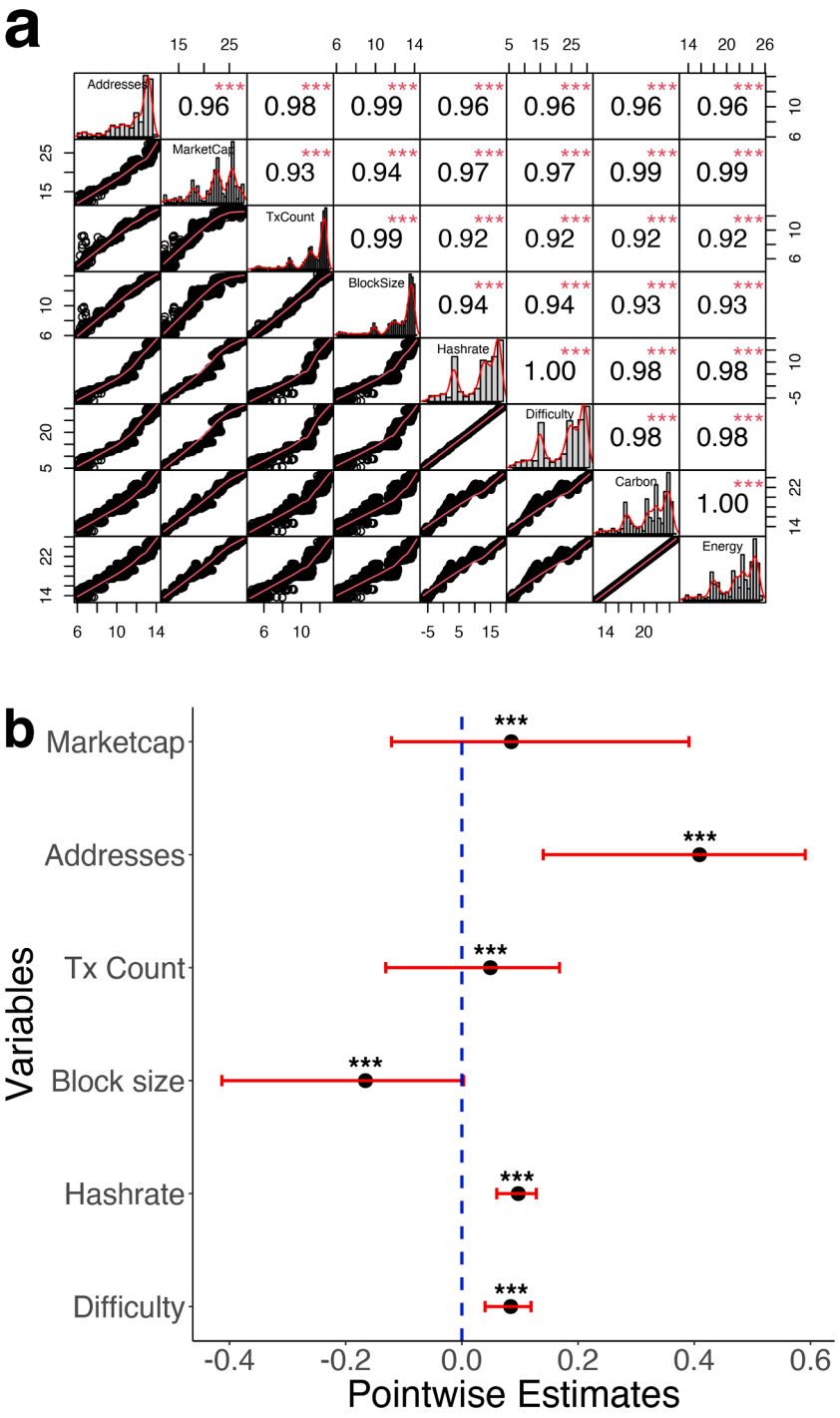

Fig. 4. Nexus between BTC carbon footprint, difficulty, hashrate, block size, transaction count, addresses, and market capitalization (a) Statistical analysis using Pearson's correlation (b) Pointwise estimates using machine learning-based regression technique. Note: *** denotes *p-value*<0.001, obs # = 4158, Lambda = 5.2, Tolerance = 0.01, Sigma = 6, Eff. Df = 13.02, R^2 = 0.985, and Looloss = 195.6.

size improves transaction efficiency and then reduces Bitcoin's energy and carbon footprint.

In the neural predictive technique, we first assessed the importance of sampled variables for the model using the "variable importance of projection (VIP)", which is synonymous with the general-to-specific modeling in econometrics (Campos et al., 2005). The VIP technique ensures that sampled variables (specifically the predictors of Bitcoin carbon footprint) that do not satisfy the requirement of VIP>0.80 are dropped from the neural predictive model. Evidence from Fig. 5(a) shows all variables are above the threshold (VIP>0.80). The importance of variables is in the order of hashrate > difficulty > market capitalization > addresses > block size > tx count. This order of importance corroborates the results of the estimated bias-corrected cross-wavelet coherence. Consequently, we used two hidden layer structures—where layer one has 3 hidden nodes while the second layer has 6 hidden nodes—with TanH activation function (due to its better performance in multilayer networks) and KFold (i.e., we used 5) as validation technique. We improved the fitting option by using robust fit and transformed covariates. The architecture of the neural network model is depicted in Fig. 5(b). The KRLS shows statistically robust results with a predictive

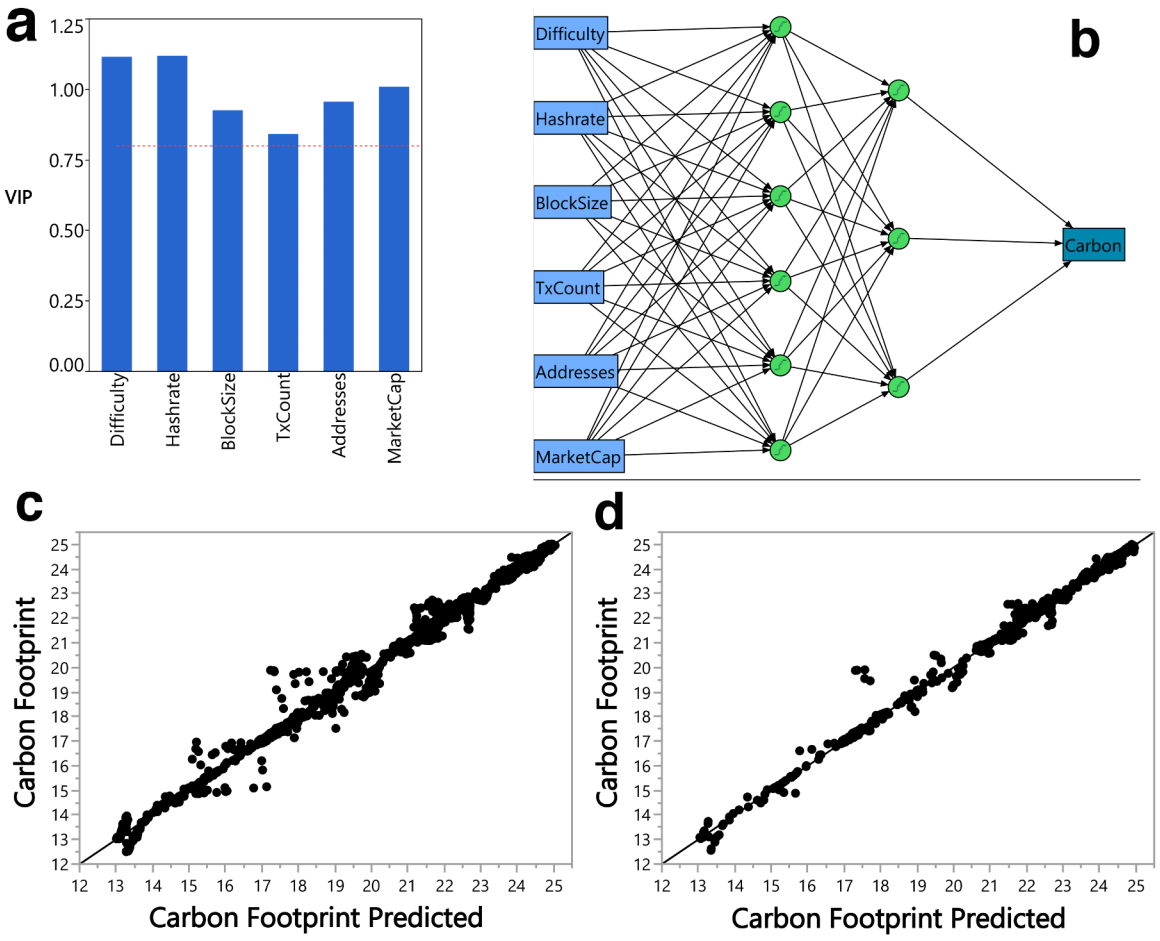

Fig. 5. Model (a) Variable importance of projection [VIP] (b) Neural network diagram (c) Training (d) Validation. Training: $R^2 = 0.997$, RMSE = 0.240, Mean Abs Dev = 0.124, -LogLikelihood = −1305.358, SSE = 191.915, and Sum Freq = 3327. Validation: $R^2 = 0.997$, RMSE = 0.259, Mean Abs Dev = 0.124, -LogLikelihood = −325.224, SSE = 55.787, and Sum Freq = 831.

power (R^2) of 98.5% whereas the training and validation models of the neural network show a higher predictive power of 99.7% (Fig. 5(c-d)).

Table 1
Hyperparameter tuning, model results, and evaluation.

(a) Tuned parameters for the model	
Parameter	Value
Epoch	50
No. of prior steps	10
No. of filters	64
Learning rate	1×10^{-4}

(b) The detailed configuration of the model						
Layer	NF*	Padding*	RFS*	AF*	NN*	DR..*
ConvLSTM2D	64	Same	1 × 1	ReLU		
Dropout						0.3
Flatten						
Dense					32	
Dense				linear	1	

(c) Models' comparison		
Model	RMSLE Energy consumption	RMSLE Carbon emissions
Vanilla LSTM	0.12	0.1
CNN-LSTM	0.05	0.06
Encoder-decoder LSTM	0.07	0.08
ConvLSTM2D	0.04	0.03
The Prophet**	1.3×10^{-6}	1.7×10^{-6}

* Note: NF = number of filters, RFS = Receptive field size, AF = activation function, NN = number of neurons, and DR.. = dropout rate.

** two multivariate time series models are developed using the Prophet package that predicts the targets with the independent variables.

We utilized Python 3.7 and TensorFlow to build the ConvLSTM2D model in this paper. The hyperparameters are adjusted by the grid search method, and the ConvLSTM model is trained and proposed, with evaluation results presented. The dataset is split into three parts namely the training set (80%), validation set (10%), and test set (10%). The grid search technique is used to compute the best hyperparameter values. Model parameter values are searched exhaustively based on their specific values, with the best hyperparameters reported. The best values of the hyperparameters and the ConvLSTM model configuration are presented in Table 1(a-b). For two multistep univariate time series problems, the ConvLSTM2D model for two targets (Bitcoin energy consumption and carbon emissions) is trained. This model utilizes the ten previous steps (t-1, t-10) of target variables as input and predicts the target variable in the time step (t). Various deep learning architectures were constructed including an encoder-decoder recurrent neural network, a CNN-LSTM, a vanilla LSTM, and ConvLSTM2D. The ConvLSTM2D model was selected among the other models based on a comparison using the RMSLE metric (Table 1(c)). Deep learning models typically suffer from overfitting issues, especially in time series, hence, the dropout technique is added to the ConvLSTM2D layer (Ismail Fawaz et al., 2019). The training and validation process is displayed in Fig. 6(a, b) for both targets. The comparison of the model prediction and the validation data for both targets is shown in Fig. 7(a,b), which shows the trained model has remarkable performance.

Subsequently, two multivariate time series problems are trained using the Prophet package (Taylor et al., 2018) with targets (energy

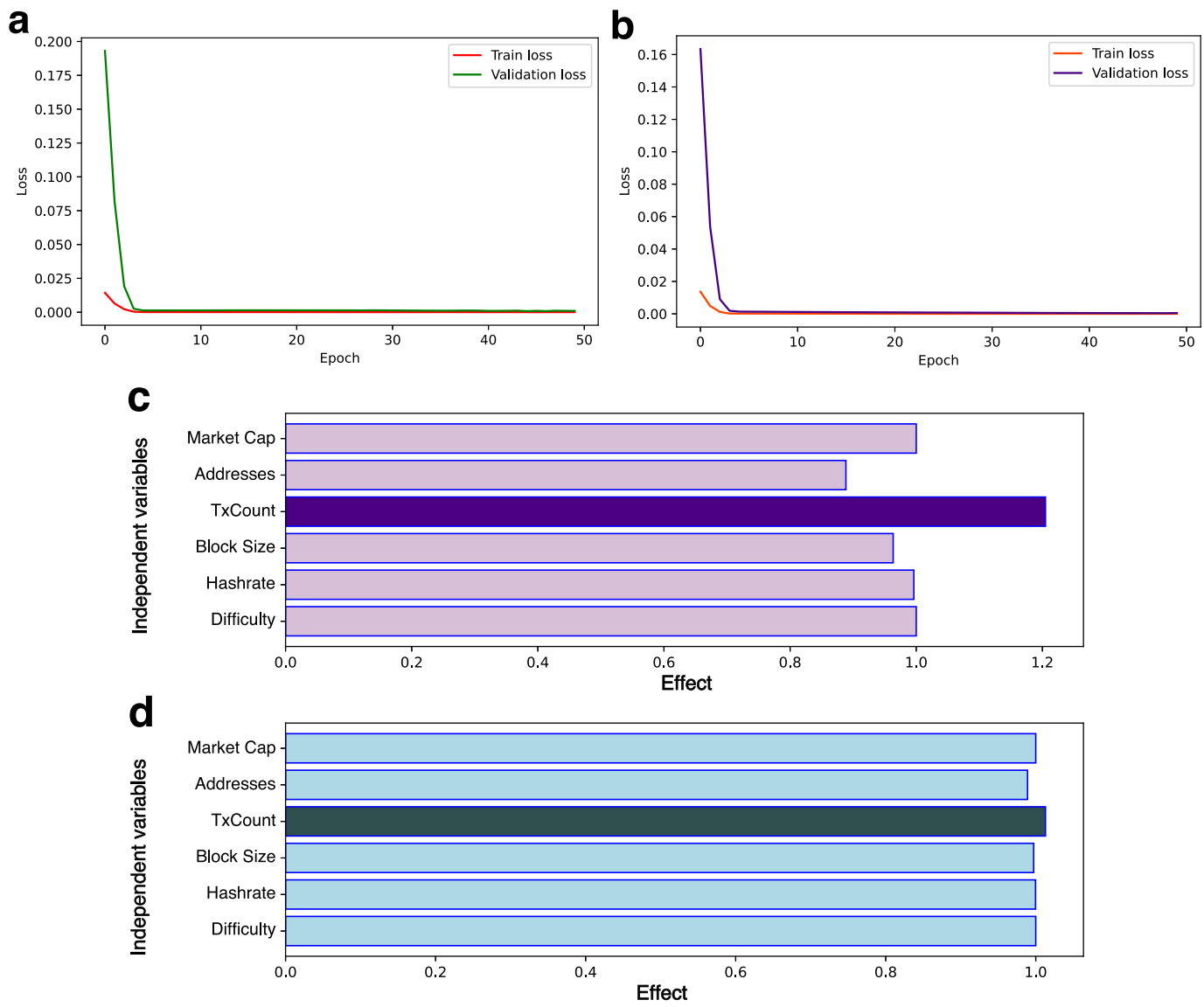

Fig. 6. The model training and validation process of ConvLSTM2D model (a) Electricity consumption (b) Carbon emissions. Feature importance of the Prophet's model (c) Electricity consumption (d) Carbon emissions.

consumption and carbon emissions) and independent variables such as difficulty, hashrate, block size, tx count, addresses, and market capitalization. Fig. 7(c,d) shows the results of the models. The evaluated models using the RMLSE metric show outstanding proficiency (Table 1 (c)). The feature importance technique is utilized to illustrate the impact of each independent variable on the dependent variable (Fig. 6(c,d)). This method is used to determine the most influential variables useful for policy-makers on decisions that increase productivity and decrease costs.

4. Discussion & conclusion

In this study, we examined the effect of Bitcoin's technical drivers on carbon footprint from an ecological perspective, useful for developing environmental policies and regulations. We further identified Bitcoin's emission sources and their potential impact on climate change. We used machine learning and econometric techniques to analyze the historical changes in Bitcoin's carbon footprint with daily data spanning July 18, 2010 to December 04, 2021. We reported the technical drivers, decomposition effects, causal relationships, and implications of the Bitcoin blockchain's increasing energy and carbon footprint. The decomposition properties were assessed using the cross-wavelet bias-corrected method to assess the temporal evolution of nonperiodic and transitory characteristics of Bitcoin's carbon footprint and technical drivers. We employed the TVGC technique with a recursive rolling window testing technique to examine the predictive power of drivers underpinning Bitcoin's carbon footprint while accounting for time-frequency variations and the timing of changes using date-stamping scenarios. We used the KRLS machine learning-based regression model to investigate the effects of Bitcoin's technical drivers on carbon footprint while controlling for misspecification bias, nonlinearity, heterogeneity, and interactive effects. Finally, two ConvLSTM2D models are proposed that can predict Bitcoin energy consumption and carbon emissions. These models forecast the targets at current times based on their ten previous steps. Due to the utilization of the dropout technique and the selection of appropriate architecture for constructing the deep learning models, our subsequent models have no overfitting problems and show proper performance in the prediction process as shown in Fig. 6(a,b). The constructed models for bitcoin energy consumption and carbon emissions are assessed with the RMSLE metric (0.04 and 0.03,

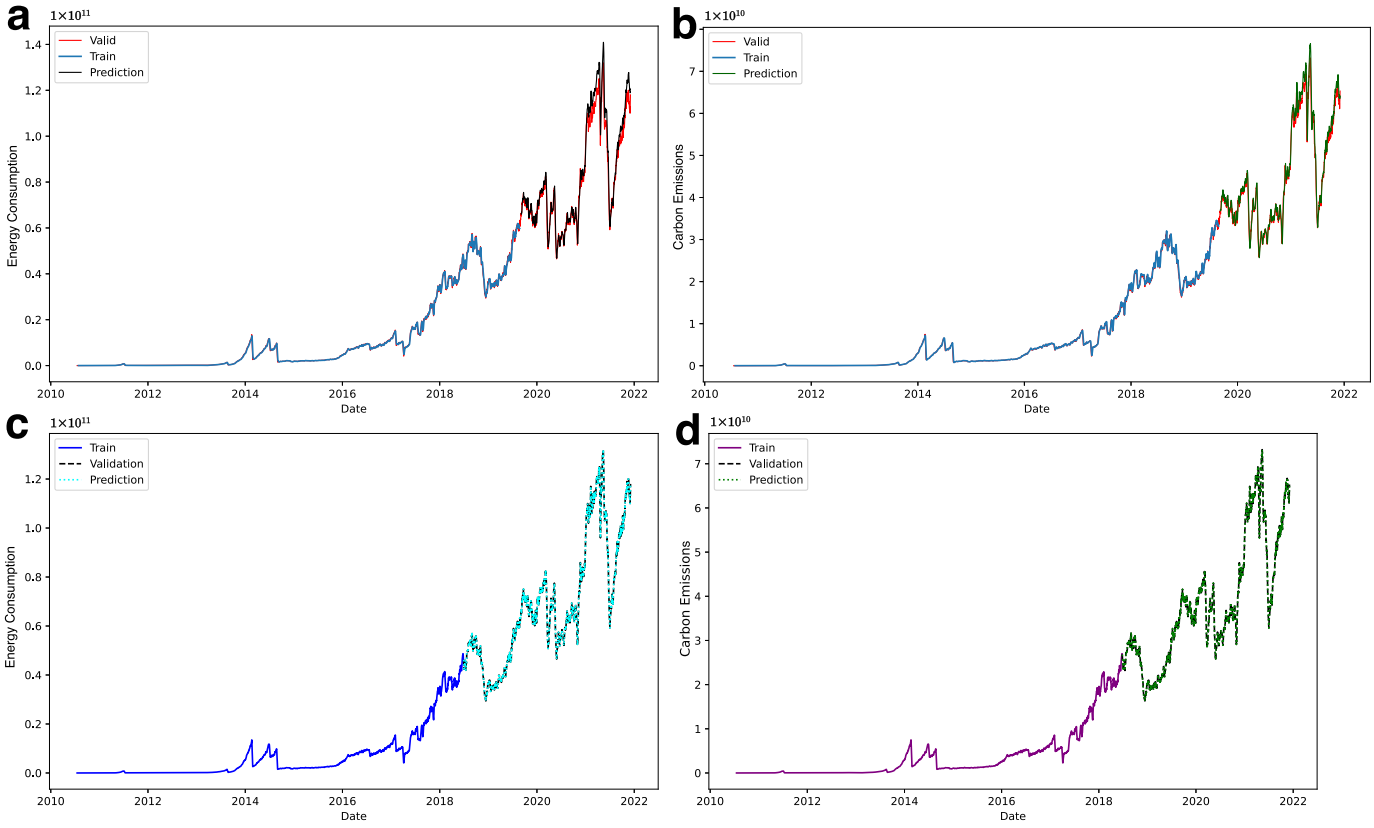

Fig. 7. The comparison of ConvLSTM2D model prediction and validation from (a) Electricity consumption (b) Carbon emissions. Comparison of Prophet's model prediction and validation from (c) Electricity consumption (d) Carbon emissions.

respectively) that show great performance. Besides, two multivariate time series Prophet models are presented that predict the targets based on the independent variables. These models reveal statistically sound results illustrated in Fig. 7(c,d), and Table 1(c). The feature importance method indicates that the number of transaction counts has the most influential effect on the targets among the other variables. It is estimated that one single Bitcoin transaction consumes as much energy as several hundred thousand VISA card transactions in 2022 (Best, 2022).

The empirical assessment shows Bitcoin's technical drivers spur Bitcoin's energy and carbon footprint. We found a strong relationship between the network hashrate and mining difficulty. The computing power required for Bitcoin PoW has quadrupled within the span of twelve months compared to the previous months of 2019. The major driver of this substantial growth is the increased difficulty in mining Bitcoin (Corbet et al., 2021). The mining difficulty is referred to as a stringent measure for a miner to generate a hashrate lower than the desired hashrate by numerically reducing the hash block head value. The mining difficulty is re-adjusted automatically upward or downward after bitcoin mining—based on the number of mining rigs and the total hash power of the mining network. The difficulty of mining increases as more miners join the network and the guesses per second increase in solving the cryptographical puzzle in a bid for block rewards (O'Dwyer et al., 2014). Thus, when the mining difficulty of the network increases, the hash power increases and vice versa. It is worth noting that the number of miners using the network, the difficulty of mining, and the profitability of mining are directly impacted by changes in hash power (Clark et al., 2019). To the bitcoin investor, the hash power is an important indicator of the network's security against hackers. Network attacks become more expensive and challenging to undertake with higher hash power. Bitcoin network hashrate increases when a rise in an additional machine is used for mining to find a subsequent block, signaling an increase in general computational electricity use and protecting the network against cyber criminals. A decline in the network hashrate occurs when there is a fall in the number of machines used for mining, making the Bitcoin network less decentralized while exposing the network to crypto heists which endangers investor funds. Ideally, the general protection of investor funds and the balance of the blockchain community requires a larger hash power to ensure extreme difficulty in blockchain cyber-attacks. Bitcoin network hashrate is estimated to be 231.44 million total hashrate per second (TH/s) as of November 23, 2022 (Blockchain.com, 2022).

We found that low mining difficulty increases market capitalization whereas increasing mining difficulty reduces bitcoin mining profit in the long term. It is intuitive to assume that rational miners are only willing to mine on the Bitcoin network if it is profitable, which directly means without demand the value will be near zero, and miners being rational will divert their resources to other economic ventures. This premise is explicitly embedded in the algorithms of the Bitcoin PoW network as mining difficulty will be readjusted to offset the fall in value and vice versa, to mitigate the impact of electricity and hardware expenditure for mining rigs. However, in a competitive market, the manufacturers of goods and services are price-takers—as an individual, or company must accept the prevailing market price. Alternatively, this premise may not hold in the bitcoin market due to its inelastic supply, and intense competition among miners within the industry that do not prompt them to act differently. In the long run, the price of bitcoin may be related to the hashrate and the total number of computations undertaken by bitcoin miners. The Bitcoin PoW consensus may be positioned to benefit from economies of scale depending on the growth of validators. For instance, if the number of Bitcoin validator nodes rises relatively fast as the system validates more transactions, it weakens energy economies of scale. Alternatively, if the number of Bitcoin validator nodes remains constant regardless of the size of the transactions process, it strengthens energy economies of scale (Platt et al., 2021). Given Bitcoin's

decentralized nature, its energy-intensive PoW verification may migrate to places with cheap electricity rates. This reveals that electricity decarbonization could assist in mitigating bitcoin's emissions in places where electricity generated from renewables is less expensive than from fossil fuel (Mora et al., 2018). In 2021, bitcoin was worth over US$68, 000, but by summer, the supposed price was halved (Sarkodie et al., 2022). This price shock was in part due to efforts by China's Financial Stability and Development Committee to curb cryptocurrency mining in the country since May 2021 (Best, 2022). China has the highest coal consumption, thus, its efforts triggered the demand for electricity from remote mining farms—so much that idle coal mines were restarted without government approval (Best, 2022; BP, 2022). Findings from the nexus between bitcoin price and mining cost suggest how bitcoin price during a bull run directly increases mining costs due to the highly intensive energy consumption (Kristoufek, 2020). Similarly, the impact of energy consumption on the Bitcoin market suggests a dynamic relationship between Bitcoin volumes, prices, and energy consumption. The authors showed that bitcoin price and volume can predict its electricity use (Huynh et al., 2022; Sarkodie et al., 2022). Evidence from a related study of bitcoin price and carbon credit market suggests the carbon market does not Granger-cause bitcoin, but bitcoin Granger-causes carbon market in the lower quantiles (Di Febo et al., 2021). Others suggest the impact of total bitcoin energy use on bitcoin price is only statistically significant at higher regimes (Maiti, 2022).

The adoption of bitcoin by big corporations could boost the incentive to use more renewable energy to produce "green bitcoin". It is worth noting that bitcoin miners need a constant and affordable energy supply, however, renewable energy is an intermittent energy source which may therefore cause miners to end up using a steady and affordable energy source like fossil fuels (De Vries, 2019). For instance, mining does not just consume power during excess renewable energy but still requires energy during shortage which may be compensated using fossil fuels (Digiconomist, 2022). One of the setbacks of green bitcoin is that renewable energy cannot solve all the environmental footprint of bitcoin—because mining rigs generate huge e-waste from obsolete hardware used, which is estimated to be 16,442 t (De Vries, 2019). The total energy consumption of the Bitcoin network must relate to the revenue as it is intuitive for the marginal revenue to exceed the marginal cost of operation and thus, necessitate the use of cheap energy sources such as coal, crude oil, and natural gas (Erdogan et al., 2022). It is reported that the share of renewables for the Bitcoin network reduced from 41.6% to 25.1% mainly due to the crackdown on mining operations in China, where mining rigs used substantial energy sources from hydropower during the wet season, but was disrupted as miners fled to other countries like the US and Kazakhstan (Charlie, 2021). For example, in 2018 about 48% of bitcoin mining capacity emanated from Sichuan—a Chinese province where cheaper and abundance of hydropower attracted the energy-intensive industry to take advantage of the lower rate (Bendiksen et al., 2018). Energy sources for bitcoin mining in other locations were mainly gas or coal-based electricity, which increased the network's average carbon intensity of electricity consumption from 478.27 gCO2/kWh in 2020 to 557.76 gCO2/kWh in 2021 (De Vries et al., 2022). Given the scenario that 4.7% of mining activities operate in China, the annual electricity consumption is estimated at ~30.34 GWh with corresponding carbon emissions between 19.12–19.42 thousand tons (Corbet et al., 2021). Although bitcoin is famous among all the cryptocurrencies, a study indicates the estimated annual electricity use of Monero after the hard fork launched is ~645.6 GWh (Li et al., 2019).

Therefore, it is essential that policymakers develop environmental regulations or policy decisions that can limit and decrease the energy consumption and carbon emission of bitcoin and other PoW mining processes (Clark et al., 2019; Jiang et al., 2021; Truby et al., 2022). Such decisions could include carbon pricing to incentivize miners to reduce their Bitcoin-attributed carbon footprint. Second, mandating the share of renewable energy for Bitcoin mining could limit emissions associated with mining and transaction processes. Third, ensuring accountability in the blockchain industry could increase the transparency of energy used for PoW mining. Fourth, setting energy efficiency standards for blockchain hardware such as mining rigs could reduce the energy use per transaction. Finally, R&D investments into sustainable blockchain technology and innovations could lead to more green crypto mining, which will reduce energy and carbon intensity. Aside from regulatory actions, behavioral change and awareness creation of the environmental impacts of unsustainable PoW mining could improve the adoption of clean and energy-efficient technologies that could reduce carbon footprint.

Due to the limitations of this study, future research could examine blockchain technologies and innovations for reducing the energy and carbon footprint of PoW-based networks.

CRediT authorship contribution statement

Samuel Asumadu Sarkodie: Conceptualization, Formal analysis, Methodology, Software, Validation, Visualization, Writing – review & editing. **Mohammad Amin Amani:** Formal analysis, Methodology, Writing – original draft. **Maruf Yakubu Ahmed:** Writing – original draft. **Phebe Asantewaa Owusu:** Writing – original draft, Writing – review & editing.

Declaration of Competing Interest

The authors declare the following financial interests/personal relationships which may be considered as potential competing interests:

Corresponding author is Associate editor of Sustainable horizon, but was not involved in any editorial process of this submission.

Supplementary materials

Supplementary material associated with this article can be found, in the online version, at doi:10.1016/j.horiz.2023.100060.

References

Agarap, A.F. (2018). Deep learning using rectified linear units (relu). *arXiv preprint* arXiv:1803.08375.

Amani, M.A., Marinello, F., 2022. A deep learning-based model to reduce costs and increase productivity in the case of small datasets: a case study in cotton cultivation. Agriculture 12 (2), 267.

Amani, M.A., Sarkodie, S.A., 2022. Mitigating spread of contamination in meat supply chain management using deep learning. Sci. Rep. 12 (1), 1–10.

American Express. (2021). *The Powerful American Express: 2020-2021 Environmental, Social and Governance Report*. Retrieved from American Express: https://s29.q4cdn.com/330828691/files/doc_downloads/esg_resources/AXP-2020-2021-ESG-Report.pdf.

Best, R.d. (2022). Energy consumption of a Bitcoin (BTC, BTH) and VISA transaction as of April 2022. Retrieved from https://www.statista.com/statistics/881541/bitcoin-energy-consumption-transaction-comparison-visa/.

Arora, V., Shi, S., 2016. Energy consumption and economic growth in the United States. Appl. Econ. 48 (39), 3763–3773.

Baum, C.F., Hurn, S., Otero, J., 2022. Testing for time-varying Granger causality. Stata J. 22 (2), 355–378.

Baur, D.G., Oll, J., 2022. Bitcoin investments and climate change: a financial and carbon intensity perspective. Finance Res. Lett. 47, 102575.

Bendiksen, C.S., Gibbons, S., Lim, E., 2018. *The Bitcoin Mining Network-Trends, Composition, Marginal Creation Cost*. Electricity Consumption & Sources.

Blockchain.com. (2022). Bitcoin Hash Rate. Retrieved from https://www.blockchain.com/en/.

BP. (2022). Statistical Review of World Energy. Retrieved from https://www.bp.com/content/dam/bp/business-sites/en/global/corporate/pdfs/energy-economics/statistical-review/bp-stats-review-2021-full-report.pdf.

Brownlee, J. (2017). How to Convert a Time Series to a Supervised Learning Problem in Python. Retrieved from https://machinelearningmastery.com/convert-time-series-supervised-learning-problem-python/.

Campos, J., Ericsson, N.R., & Hendry, D.F. (2005). General-to-specific modeling: an overview and selected bibliography. *FRB International Finance Discussion Paper*(838).

Capgemini. (2018). *WORLD PAYMENTS REPORT 2018*. Retrieved from BNP Paribas: https://worldpaymentsreport.com/wp-content/uploads/sites/5/2018/10/World-Payments-Report-2018.pdf.

Cazelles, B., Chavez, M., Magny, G.C.d., Guégan, J.-F., Hales, S., 2007. Time-dependent spectral analysis of epidemiological time-series with wavelets. J. Roy. Soc. Interface 4 (15), 625–636.

Cazelles, B., Chavez, M., Berteaux, D., Ménard, F., Vik, J.O., Jenouvrier, S., Stenseth, N. C., 2008. Wavelet analysis of ecological time series. Oecologia 156 (2), 287–304.
CBECI. (2021). Cambridge Bitcoin Electricity Consumption Index. Retrieved from https://ccaf.io/cbeci/index/.
Charlie, C., 2021. Why China Is Cracking Down on Bitcoin Mining and What It Could Mean for Other Countries. Time. Retrieved from. https://buff.ly/3JbhpCX.
Clark, C.E., & Greenley, H.L. (2019). *Bitcoin, blockchain, and the energy sector*: Congressional Research Service.
CMC. (2022). Coin Market Capitalization Retrieved from https://coinmarketcap.com/.
Coin Metrics. (2022). Data File Downloads - Coin Metrics. Retrieved from https://coinmetrics.io/community-network-data/#.
Coin Desk. (2022). White House Calls for Crypto Mininig Standard to Minimize Environmental Impact Retrieved from https://www.coindesk.com/.
Digiconomist. (2022). Bitcoin Energy Consumption Index. Retrieved from https://digiconomist.net/bitcoin-energy-consumption/.
Corbet, S., Lucey, B., Yarovaya, L., 2021. Bitcoin-energy markets interrelationships-New evidence. Resour. Policy 70, 101916.
De Vries, A., Gallersdörfer, U., Klaaßen, L., Stoll, C., 2022. Revisiting Bitcoin's carbon footprint. Joule 6 (3), 498–502.
De Vries, A., 2019. Renewable energy will not solve bitcoin's sustainability problem. Joule 3 (4), 893–898.
DeBoef, S., Granato, J., 1997. Near-integrated data and the analysis of political relationships. Am. J. Pol. Sci. 619–640.
Di Febo, E., Ortolano, A., Foglia, M., Leone, M., Angelini, E., 2021. From Bitcoin to carbon allowances: an asymmetric extreme risk spillover. J. Environ. Manage. 298, 113384.
Erdogan, S., Ahmed, M.Y., Sarkodie, S.A., 2022. Analyzing asymmetric effects of cryptocurrency demand on environmental sustainability. Environ. Sci. Pollut. Res. 29 (21), 31723–31733.
Ferwerda, J., Hainmueller, J., Hazlett, C.J., 2017. Kernel-based regularized least squares in R (KRLS) and Stata (krls). J. Stat. Softw. 79 (3), 1–26.
Grinsted, A., Moore, J.C., Jevrejeva, S., 2004. Application of the cross wavelet transform and wavelet coherence to geophysical time series. Nonlinear Process Geophys. 11 (5/6), 561–566.
Hainmueller, J., Hazlett, C., 2014. Kernel regularized least squares: reducing misspecification bias with a flexible and interpretable machine learning approach. Politi. Analy. 22 (2), 143–168.
Hobijn, B., Franses, P.H., Ooms, M., 2004. Generalizations of the KPSS-test for stationarity. Stat. Neerl. 58 (4), 483–502.
Huynh, A.N.Q., Duong, D., Burggraf, T., Luong, H.T.T., Bui, N.H., 2022. Energy consumption and Bitcoin market. Asia-Pac. Financ. Mark. 29 (1), 79–93.
IMF. (2022). *Digital Currencies and Energy Consumptions*. Retrieved from IMF: https://www.imf.org/en/Publications/fintech-notes/Issues/2022/06/07/Digital-Currencies-and-Energy-Consumption-517866.
Ismail Fawaz, H., Forestier, G., Weber, J., Idoumghar, L., Muller, P.-A., 2019. Deep learning for time series classification: a review. Data Min. Knowl. Discov. 33 (4), 917–963.
Iyer, T., 2022. Cryptic connections: Spillovers Between Crypto and Equity Markets. International Monetary Fund.
Jiang, S., Li, Y., Lu, Q., Hong, Y., Guan, D., Xiong, Y., Wang, S., 2021. Policy assessments for the carbon emission flows and sustainability of Bitcoin blockchain operation in China. Nat. Commun. 12 (1), 1–10.
Köhler, S., Pizzol, M., 2019. Life cycle assessment of bitcoin mining. Environ. Sci. Technol. 53 (23), 13598–13606.
Kagalwala, A., 2022. kpsstest: a command that implements the Kwiatkowski, Phillips, Schmidt, and Shin test with sample-specific critical values and reports p-values. Stata J. 22 (2), 269–292.
Kristoufek, L., 2020. Bitcoin and its mining on the equilibrium path. Energy Econ. 85, 104588.
Kwiatkowski, D., Phillips, P.C., Schmidt, P., Shin, Y., 1992. Testing the null hypothesis of stationarity against the alternative of a unit root: how sure are we that economic time series have a unit root? J. Econom. 54 (1–3), 159–178.
Lau, K.-M., Weng, H., 1995. Climate signal detection using wavelet transform: how to make a time series sing. Bull. Am. Meteorolog. Soc. 76 (12), 2391–2402.
Li, J., Li, N., Peng, J., Cui, H., Wu, Z., 2019. Energy consumption of cryptocurrency mining: a study of electricity consumption in mining cryptocurrencies. Energy 168, 160–168.
Maiti, M., 2022. Dynamics of bitcoin prices and energy consumption. Chaos, Solitons & Fractals: X 9, 100086.
Mallat, S., 1999. A Wavelet Tour of Signal Processing. Elsevier.
Master Card. (2021). *Corporate Sustainaability Report 2020*. Retrieved from https://www.mastercard.us/content/dam/public/mastercardcom/na/global-site/documents/mastercard-sustainability-report-2020.pdf.
O'Dwyer, K.J., & Malone, D. (2014). Bitcoin mining and its energy footprint.
McCook, H., 2014. An order-of-magnitude estimate of the relative sustainability of the Bitcoin network. A Criti. Assess. Bitcoin Mini. Indus. Gold Product. Indus Leg. Bank. Syst. Product. Phys. Curr. 2, 25.
Mora, C., Rollins, R.L., Taladay, K., Kantar, M.B., Chock, M.K., Shimada, M., Franklin, E. C., 2018. Bitcoin emissions alone could push global warming above 2 C. Nat. Clim. Chang. 8 (11), 931–933.
Nakamoto, S., 2008. Bitcoin: a peer-to-peer electronic cash system. Decentral. Bus. Rev. 21260.
Platt, M., Scdlmeir, J., Platt, D., Xu, J., Tasca, P., Vadgama, N., Ibañez, J.I., 2021. The energy footprint of blockchain consensus mechanisms beyond proof-of-work. In: Paper presented at the 2021 IEEE 21st International Conference on Software Quality, Reliability and Security Companion (QRS-C).
Sarkodie, S.A., Owusu, P.A., 2020. How to apply the novel dynamic ARDL Simulations (dynardl) and Kernel-based Regularized Least Squares (krls). MethodsX, 101160. https://doi.org/10.1016/j.mex.2020.101160.
Sarkodie, S.A., Owusu, P.A., 2022. Dataset on bitcoin carbon footprint and energy consumption. Data Bri. 42, 108252 https://doi.org/10.1016/j.dib.2022.108252.
Sarkodie, S.A., Ahmed, M.Y., Leirvik, T., 2022a. Trade volume affects bitcoin energy consumption and carbon footprint. Finance Res. Lett. 48, 102977 https://doi.org/10.1016/j.frl.2022.102977.
Sarkodie, S.A., Ahmed, M.Y., Owusu, P.A., 2022b. COVID-19 pandemic improves market signals of cryptocurrencies–evidence from Bitcoin, Bitcoin Cash, Ethereum, and Litecoin. Finance Res. Lett. 44, 102049 https://doi.org/10.1016/j.frl.2021.102049.
Schwarz, G., 1978. Estimating the dimension of a model. Ann. Statist. 461–464.
Shi, X., Chen, Z., Wang, H., Yeung, D.-Y., Wong, W.-K., Woo, W.-c, 2015. Convolutional LSTM network: a machine learning approach for precipitation nowcasting. Adv. Neural Inf. Process. Syst. 28.
Shi, S., Hurn, S., Phillips, P.C., 2020. Causal change detection in possibly integrated systems: revisiting the money–income relationship. J. Financ. Econometr. 18 (1), 158–180.
Srivastava, N., Hinton, G., Krizhevsky, A., Sutskever, I., Salakhutdinov, R., 2014. Dropout: a simple way to prevent neural networks from overfitting. J. Mach. Learn. Res. 15 (1), 1929–1958.
Stoll, C., Klaaßen, L., Gallersdörfer, U., 2019. The carbon footprint of bitcoin. Joule 3 (7), 1647–1661.
Swanson, N.R., 1998. Money and output viewed through a rolling window. J. Monet. Econ. 41 (3), 455–474.
Taylor, S.J., Letham, B., 2018. Forecasting at scale. Am. Stat. 72 (1), 37–45.
Truby, J., Brown, R.D., Dahdal, A., Ibrahim, I., 2022. Blockchain, climate damage, and death: policy interventions to reduce the carbon emissions, mortality, and net-zero implications of non-fungible tokens and Bitcoin. Energy Res. Soc. Sci. 88, 102499 https://doi.org/10.1016/j.erss.2022.102499.
Visa. (2020). *2020 Environmental, Social & Governance Report*. Retrieved from Visa: https://usa.visa.com/content/dam/VCOM/global/about-visa/documents/visa-2020-esg-report.pdf.
Wang, Y., Sun, L., Peng, D., 2022. A Multihead ConvLSTM for Time Series Classification in eHealth Industry 4.0. Wirel. Commun. Mob. Comput. *2022*.
WB. (2018). Global Payment System Survey (GPSS). Retrieved from https://www.worldbank.org/.
WHG. (2022). *Climate and Energy Implications of Crypto-Assets in the United States*. Retrieved from whitehouse.gov: https://www.whitehouse.gov/.

Samuel Asumadu Sarkodie is a multidisciplinary researcher with Ph.D. in Environmental Sciences from Macquarie University (Australia). He was recognized by Clarivate–Web of Science as a Highly Cited Researcher in Environment & Ecology (in 2022) and Cross-field (in 2021). He's currently a research fellow at Nord University, Norway. His-research interest includes environmental and energy economics, environmental health, environmental modeling, environmental policy, climate change, health impact assessments, sustainable development, air pollution, and sustainable management of the environment. He has >100 peer-reviewed S/SCI-E journal articles and currently serves as a subject editor for Sustainable Production and Consumption (Elsevier), Sustainability (MDPI), and Earth (MDPI)—and Associate Editor for Sustainable Horizons (Elsevier), Heliyon (CellPress), and Frontiers in Environmental Science (Frontiers).

Mohammad Amin Amani is a research assistant in the Industrial Engineering department at the University of Tehran, Iran. He did his master's degree in Industrial Engineering at the College of Engineering, University of Tehran in Iran. His-research interests comprise machine learning, deep learning, robust optimization, stochastic programming, logistics, and applied operations research.

Maruf Yakubu Ahmed is a Ph.D. candidate in finance at the University of Vaasa Finland. His-research interests include several areas of financial economics such as commodity market, fintech, sustainable finance, and environmental sustainability.

Phebe Asantewaa Owusu is a researcher with MS in Sustainable Environmental and Energy Systems. She's currently a Ph.D. candidate in Business at Nord University, Norway. Her research interests include environmental health, modeling, climate change, health impact assessments, sustainable development, and air pollution. She has >50 peer-reviewed S/SCI-E journal articles.